Available online at www.sciencedirect.com
SCIENCE DIRECT
Marine and Petroleum Geology 23 (2006) 529–542
Marine and Petroleum Geology
www.elsevier.com/locate/marpetgeo

Restudy of acid-extractable hydrocarbon data from surface geochemical survey in the Yimeng Uplift of the Ordos Basin, China: Improvement of geochemical prospecting for hydrocarbons

Liuping Zhang[a,*], Guoping Bai[b], Kebin Zhao[c], Changqing Sun[c]

[a]*Key Laboratory of Petroleum Resource, Institute of Geology and Geophysics, Chinese Academy of Sciences, P.O. Box 9825, Beijing 100029, PR China*
[b]*Basin & Reservoir Research Center, China University of Petroleum, Beijing 102249, PR China*
[c]*Research Institute of Petroleum Exploration and Development, SinoPec, Beijing 100083, PR China*

Received 5 January 2006; received in revised form 5 April 2006; accepted 24 April 2006

Abstract

Two geochemical surveys were conducted in 1992 and 2000 respectively in the Yimeng Uplift of the Ordos Basin, China. The earlier survey grid had 1×5 km spacing and the later survey grid had 0.5×0.5 km spacing. The acid-extractable hydrocarbons of both surveys show similar geochemical trends. However, the anomalies obtained with traditional statistical methods do not correlate with existing oil/gas fields. This study reveals two problems in the data and their processing. The first one is interference caused by the variation of soil composition. We applied a wavelet-analysis-based method to eliminate this interference in the data of the later survey. The second is that micro-seepage anomalies did not identify existing oil/gas fields and seepage anomalies related with faults had not been previously recognized. We modified the logic multiplication cluster analysis and applied a multi-fractal model and a back propagation artificial neural network to recognize these two types of anomalies that cannot be recognized with typical statistics in the study area. The recognized seepage anomalies display a string-bead-shaped pattern and some are distributed along a large fault in this area. The fault is the main pathway for hydrocarbon migration. The micro-seepage anomalies are ring-shaped and are mostly distributed close to the fault. They coincide with oil/gas field and structure traps. Therefore, reprocessing of existing geochemical data using these new methods can greatly improve their usefulness in hydrocarbon exploration.

Keywords: Hydrocarbons; Geochemical exploration; Interference; Anomalies; Data processing

1. Introduction

The analytical method for acid-extractable hydrocarbons occluded in soils was developed in 1930s (Horvitz, 1939, 1972, 1985). Since then, this method has become common in surface geochemical exploration and plenty of data derived from it have accumulated throughout the world. However, it commonly suffers from the interference caused by variation of soil composition (Horvitz, 1985; Ruan and Cheng, 1991; Abrams, 2005). Because of this, some geochemical signatures are not considered to be distinguishable from background sediment signals with current methods used by industry (Abrams, 2005). This could be one of the many reasons why geochemical hydrocarbon exploration still remains an unconventional approach in the petroleum industry, although geochemical hydrocarbon exploration was systematically studied back in 1929 (Davidson, 1994; Saunders et al., 1999). To improve the application of these data to hydrocarbon prospecting, we have studied the data-processing methods since 1990s, which include interference elimination and anomaly recognition. Although the methods for anomaly recognition were developed on the basis of typical statistics (Zhang, 1993; Zhang and Liao, 1998), they sometimes cannot be used because the data do not meet the prerequisite of typical statistics (normal distributions of

*Corresponding author. Tel.: +86 10 6200 7374; fax: +86 10 6201 0846.
E-mail addresses: lpzhang_int@hotmail.com (L. Zhang), baigp@cup.edu.cn (G. Bai).

0264-8172/$ - see front matter © 2006 Elsevier Ltd. All rights reserved.
doi:10.1016/j.marpetgeo.2006.04.003

multi-population) or cannot be separated into background and anomalies by probability graph. This paper presents a case study in the Yimeng Uplift of the Ordos Basin in central China, which involves undefinable anomalies because the anomalies cannot be properly recognized with traditional statistic methods. To solve this problem, we applied a wavelet-analysis-based method (Zhang et al., 2003) for interference elimination, employed the multi-fractal model (Cheng et al., 1994; Cheng, 1999) for univariate recognition, improved logic multiplication cluster anlysis and utilized back propagation artificial neural network (Zhang and Bai, 2002) for multi-variate anomaly recognition in this paper, and achieved a better result than previous studies. This paper illustrates that the integrated application of these new methods can greatly improve the predictive capability of the existing data.

2. Background and previous work

The Ordos Basin is situated in central China, limited by latitudes 34:00°N–40:35°N and by longitudes 106:50°E to 111:10°E, with an area of 250,000 km^2 (Fu et al., 2001). It is divided into six structural units: Yimeng uplift, Weibei uplift, Western edge thrusting belt, Jinxi flexural fold belt, Tianhuan depression and Shanbei slope. Three giant gas fields, Jingbian in Ordovician carbonates, Yulin and Suligemiao in Lower Permian clastics, have been found on the Shanbei slope. The study area is located in the Yimeng Uplift and lies north of the Yulin Gas Field (Fig. 1).

The basement of the Ordos Basin consists of Archean and Proterozoic metamorphics and the sedimentary cover is composed of Paleozoic to Cenozoic sequences (Yang et al., 1992; Ritts et al., 2004; Fig. 2). Beneath the Ordovician weathered crust are cryptite, algae-bearing dolomite, pelitic limestone and shale, which have a thickness of 50–500 m. The Ordovician rocks are widespread across the basin (Fu et al., 2001).

Due to depositional hiatus and erosion, the Upper Ordovician to the Lower Carboniferous sequences is not preserved in the basin (Fig. 2). The Carboniferous contains marine and non-marine clastic rocks and carbonates, and the Permian is dominated by non-marine clastics. The

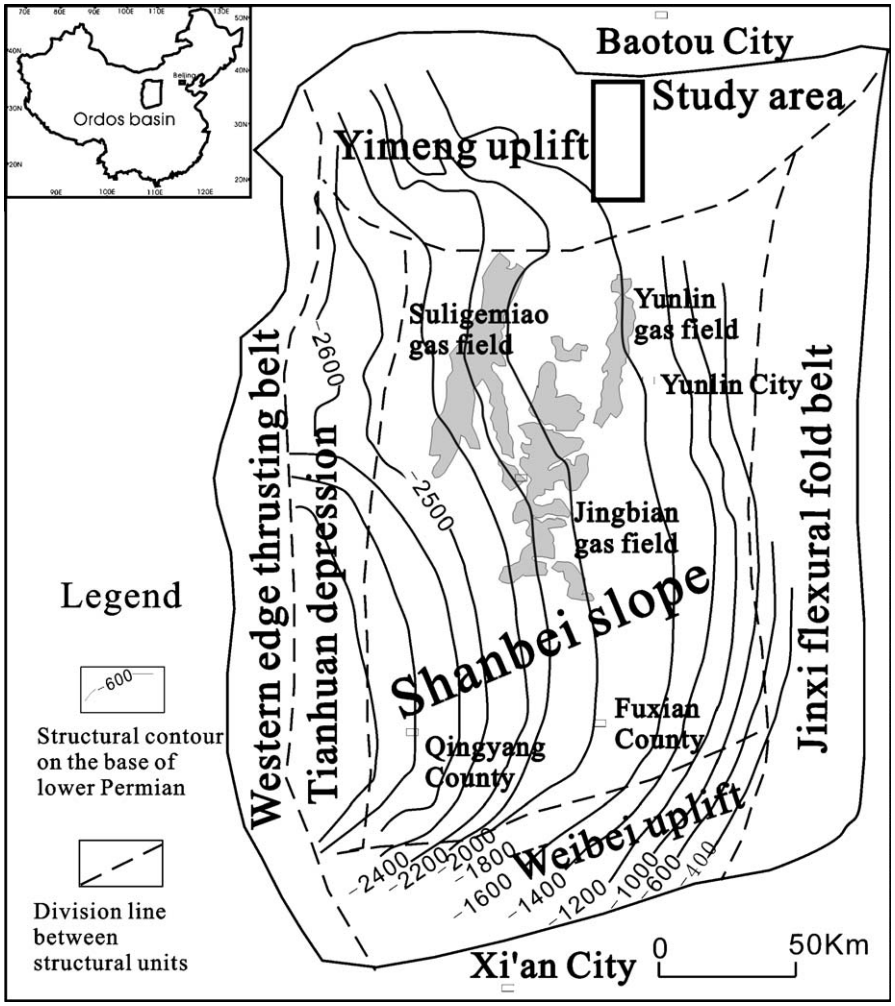

Fig. 1. Structural contour to the base of Lower Permian (in meters below sea level) of the Ordos Basin as well as the location of the study area (after Zhang and Chang (2002)).

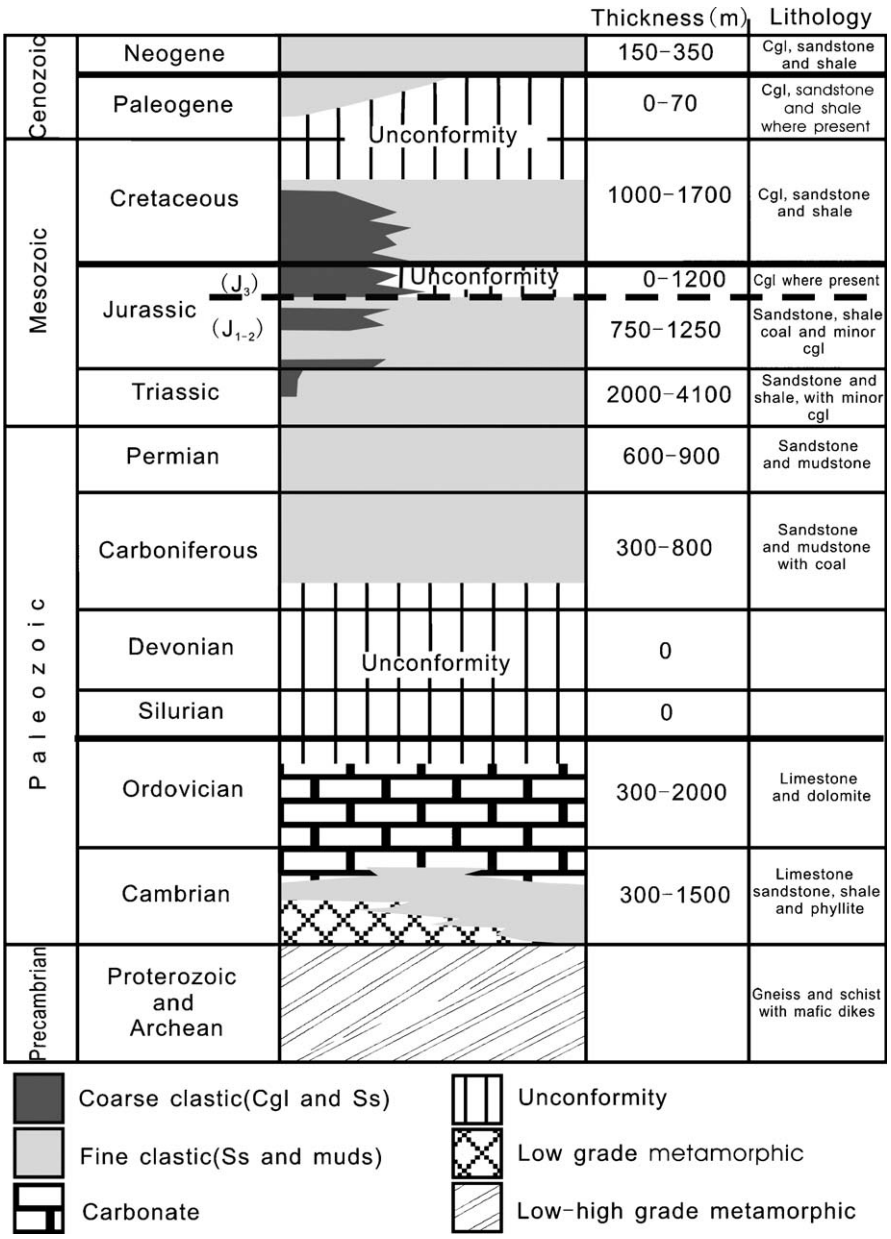

Fig. 2. Generalized stratigraphic section for the Ordos basin. Data are primarily from Yang et al. (1992) and Ritts et al. (2004), and do not represent a complete stratigraphic column for any one part of the basin.

upper Paloezoic source rocks are composed of coal, dark mudstone and limestone. Among them, coal and dark mudstone are important gas source rocks that are distributed over an area of 180,000 km^2 with a peak gas generation and migration in Early Cretaceous. Coal seams are 5–20 m thick, and dark mudstone 60–100 m with a 2–3% organic carbon content. The kerogen in these source rocks are of type III with *Ro* equal to and greater than 1.3%. The Upper Paleozoic source kitchen was located to the south of the Yulin Gas Field (Fu et al., 2001). Hydrocarbons mainly migrated along the sand bodies to the north.

The Yimeng uplift had risen since Middle Proterozoic. The Upper Carboniferous and Permian are dominated by alternated marine and terrestrial facies. The Carboniferous is composed of the Taiyuan Formation; and the Permian, the Shanxi, Xiashihezi, Shangshihezi and Shiqianfeng Formations. Within the Taiyuan Formation, sand bodies were well developed as littoral and tidal-flat facies. The sand bodies in the Shanxi Formation deposited as channel bed, fluvial channel, estuary and marginal bank facies. The sand bodies in the Xiashihezi Formation were deposited in similar environments. They are more widely distributed and are the main exploration intervals in the north part of the basin.

The Shiqianfeng Formation is mainly composed of mudstone and is considered as a regional seal for the Paleozoic hydrocarbon system (Yang et al., 2000; Li et al., 2000). The Shanxi, Xiashihezi and Shangshihezi Formations consist of interbedded sandstone and mudstone. The

mudstone layers in these formations can act as local seals for gas reservoirs.

Fig. 3 shows the structural maps for the bottom of the Carboniferous and the top of the Permian Shangshihezi Formation. Small traps are developed in this study area. The weathered crust is accidented (Fig. 3A). Deposition of Carboniferous sediments on this crust and subsequent differential compaction resulted in the formation of numerous small scale anticlines (Fig. 3B). In addition, the faulting led to the formation of small anticlines along the thrust fault (Sun et al., 2000). Nine wells were drilled in the study area. All of them have oil/gas shows. Wells Ys 1, M 1, Y 10 and Y 26 yielded commercial flows; Y18, Y19, Jp 1 and Jp2 recorded sub-commercial flow rates (Fig. 3). Following the test, the wells with commercial flow rate have not been put into production since no pipe lines are available to transport the produced gas. Therefore, there exist hydrocarbons in these fields while geochemical surveys were conducted.

The soils at the surface are Quaternary and composed of sand, clay and their mixture. The desertification of the soils is taking place because of cold and dry climate prevailing in the area. A geochemical survey was conducted with a grid of 1×5 km in 1992. Samples at a depth of 1.5 m were collected by using a twist drill. The collected samples were exposed to air for drying and then put into special packets with metal underlayers for transportation. Most samples are coarse-grained and contain relatively few materials finer than 200 mesh. Therefore, sand removal by sieving could not be used to eliminate interference that could be caused by soil composition in this area. The dry samples were briefly sieved to 40 mesh. The materials finer than 40 mesh were analyzed for acid-extractable hydrocarbons using Horvitz's approach (Horvitz, 1985; Ruan and Fei,

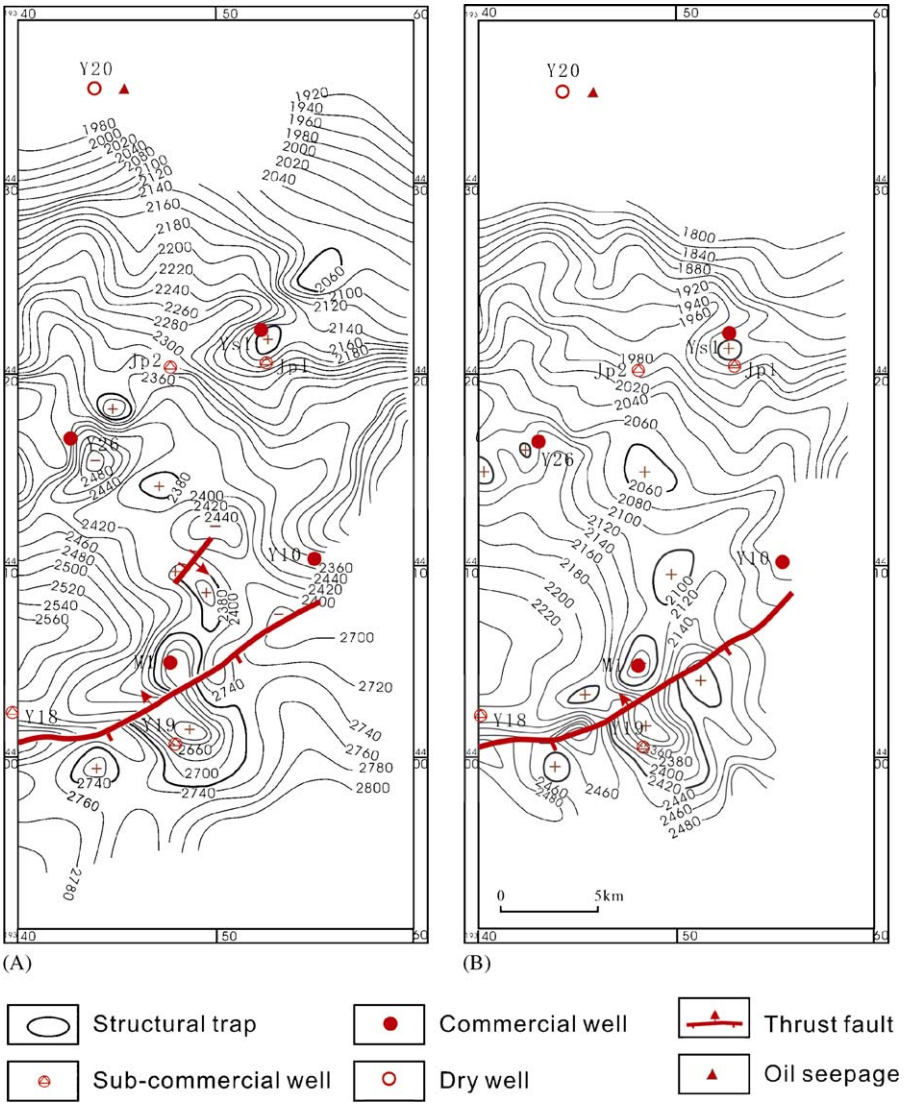

Fig. 3. Structrual contour map to the bottom of the Carboniferous (A) and the top of the Permian Shangshihezi Formation (B) in the studied area of the Yimeng uplift in the Ordos Basin, China (contours in meters below sea level; after Sun et al.. (2000)).

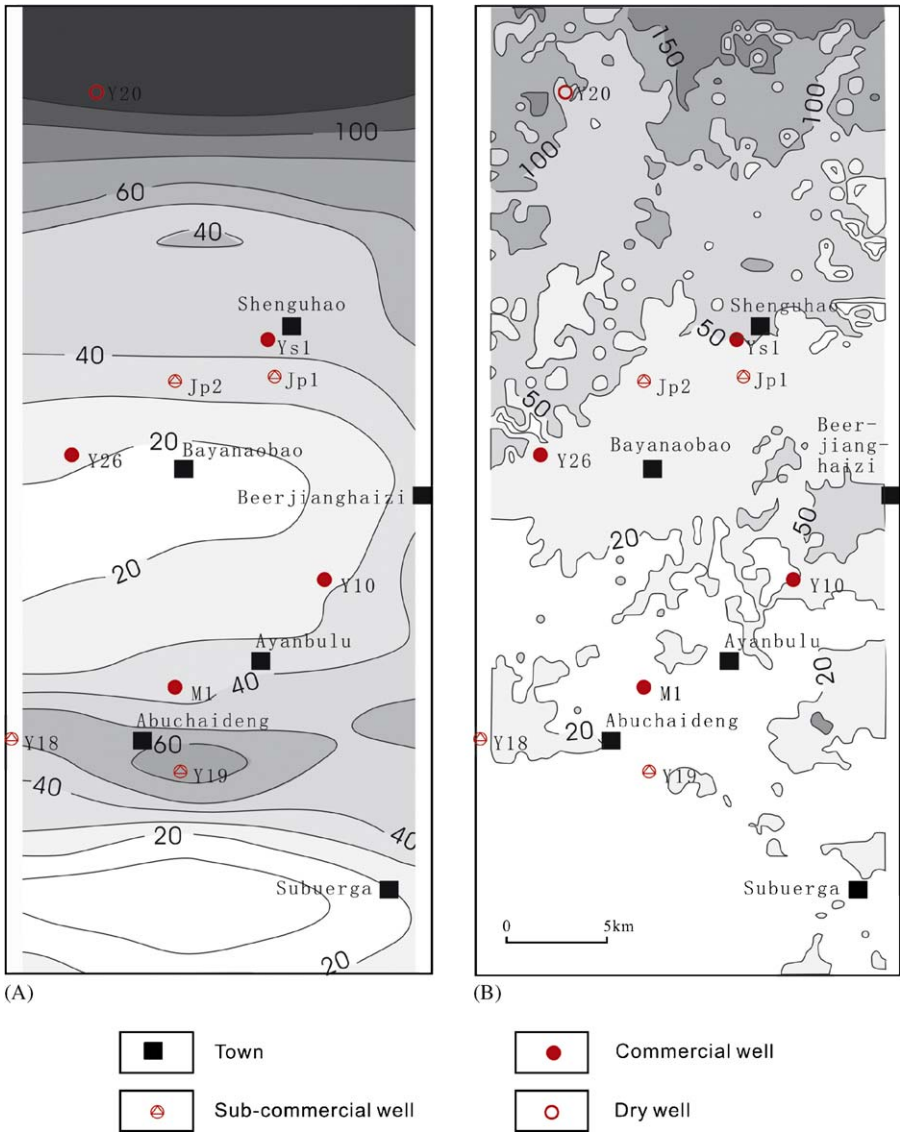

Fig. 4. Anomalies of acid-extractable CH_4 in the study area of the Yimeng uplift in the Ordos Basin, China, processed with traditional methods (from Sun et al. (2000)). (A) Anomaly map derived from survey conducted in 1992. Anomalous threshold is 60 μl/kg, (B) Anomaly map derived from survey finished in 2000. The threshold is 100 μl/kg.

1992). The fine-grained portion is heated in hydrochloric acid in a partial vacuum to remove 'bound' hydrocarbons. The anomalies with high values of acid- extractable hydrocarbons are located in the northern part of the study area and are not associated with commercial wells (Fig. 4A). It was considered that the low grid should be one of the reasons for this non-association. In 2000, another survey with a tighter grid of 0.5 × 0.5 km was carried out to check whether this kind of survey can be valuable for hydrocarbon prospecting. A total of 4095 samples were collected at a depth of 1.5 m. The same procedure was employed for the analysis of acid extractable hydrocarbons. Unexpectedly, a similar trend of geochemical distribution was obtained and is shown in Fig. 4B. However, the anomalies of both surveys do not demonstrate any association with traps and the producing wells, and they occur over large areas.

3. Interference and its elimination

Many researchers (Klusman, 1993; Ruan and Fei, 1992; Tedesco, 1995) have noticed that microorganisms can eat and/or produce hydrocarbons at the surface, causing interference in the data obtained by surface geochemical surveys. This interference is referred to as organism interference. This interference is a superimposition type based on this formation mechanism (Zhang et al., 2003). Another type of interference results from the change of soil mineral components, which is termed as soil interference. Our studies in Heibei province, Shandong province and Inner Mongolia in China indicate that soil interference is more commonly developed than organism interference. This interference results from the dilution by sand in soils or condensation by clays and/or carbonates. Therefore, the soil interference belongs to the multiplication type (Zhang et al., 2003).

Many published literatures (Klusman, 1993; Ruan and Fei, 1992; Tedesco, 1995; Gonzalez et al., 2002; Zhang et al., 2003) present that hydrocarbon anomalies are sharp peaks with high-frequency variation, even in the case where the spacing is only 10 m between sampling points on the cross-section (Xu, 1993). The large anomalies in the northern part of the study area (Fig. 4) do not coincide with the geometric nature of hydrocarbon anomalies but probably resulted from interference. Fig. 5 shows the variation of the soil characteristics. The soils of clay and sandy clay are mainly distributed in the northern part. To the south, the sand contents in soils increase. In the southern part of the study area, there exist lots of sand soils. Table 1 shows that clay soils contain more hydrocarbons than sand soils. When soils contain more sand, sand will minimize hydrocarbons absorbed and/or occluded in soils and thus result in interference. That may be the reason why the acid-extractable hydrocarbons in soils tend to decrease in abundance to the south (Figs. 4 and 5). The hydrocarbons along the survey line 25 (Figs. 5 and 6) show that the anomalies on the lower background in the southern part are much weaker than those on the higher background in the north. Compared with methane, the heavier hydrocarbon components suffer a similar or more intense interference. All of these features suggest that the

Table 1
Acid-extractable hydrocarbons in different types of soils in the study area (μl/kg)

	CH_4	C_2H_6	C_3H_8	iC_4H_{10}	nC_4H_{10}
Clay and sandy clay	125.06	12.55	4.65	1.06	1.41
Clayey sand	61.09	3.21	1.28	0.32	0.41
Sand	41.25	2.58	1.02	0.24	0.36

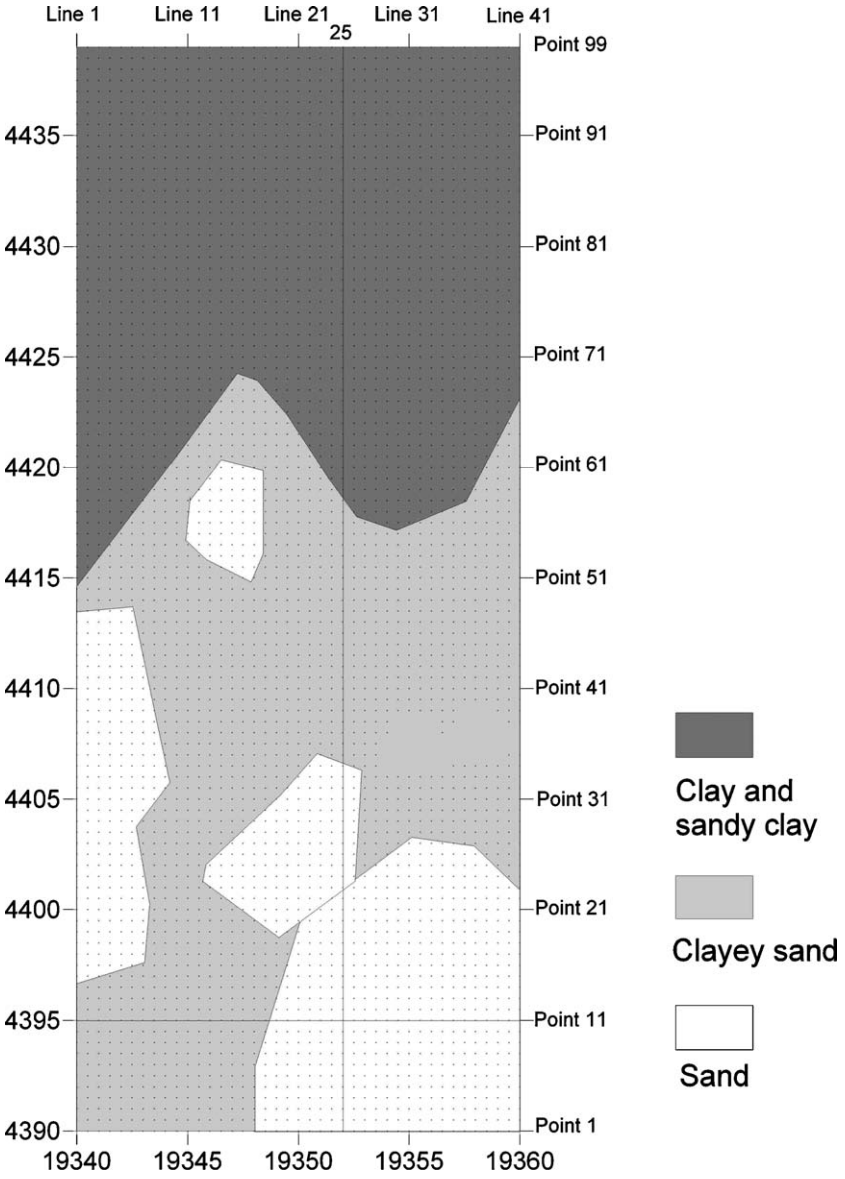

Fig. 5. Distribution of different kinds of soils in the study area of the Yimeng Uplift in the Ordos Basin, China.

interference in this area belongs to multiplication type (refer to Zhang et al., 2003). The climate of the study area is cold and dry, which is unfavorable for the survival of organisms. Thus, the organism interference (superimposition type) is unlikely to have developed.

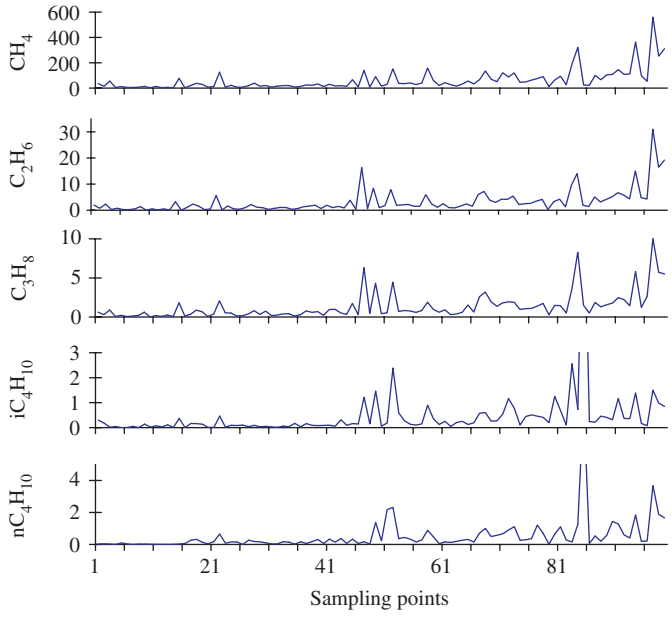

Fig. 6. Hydrocarbons occluded in soils along survey line 25 in the study area of the Ordos Basin, China.

Zhang et al. (2003) established a method based on wavelet analysis. The literature indicates that Morlet wavelet, symmetric border treatment, Mallat's algorithm and the data preprocessing for different types of interference are suitable for geochemical hydrocarbon exploration. For the interference of multiplication type, log-transformation and normalization are required before wavelet decomposition. The inverse log-normalization is carried out following the inverse wavelet transform. Wavelet analysis for the elimination of soil interference was performed for the data from the survey line 25 (Fig. 7). C4 sequence (refer to Zhang et al., 2003) hardly contains the detailed (anomalous) information so that it reflects interference signal (Fig. 7A). The values in C4 sequence were reassigned to be equal to zero. The inverse wavelet transform and then inverse log-normalization were conducted by taking the detailed information reflected by D1–D4 sequences. The results of the inversion transformation show that the data are properly corrected. The data on the lines perpendicular to the survey lines were also checked. It is further demonstrated that the interference results from the variation of soil mineral components and C4 reflects the interference. Then 2-D data of CH_4, C_2H_6, C_3H_8, iC_4H_{10} and nC_4H_{10} were processed in the same manner and in 2-D way (refer to Zhang et al., 2003).

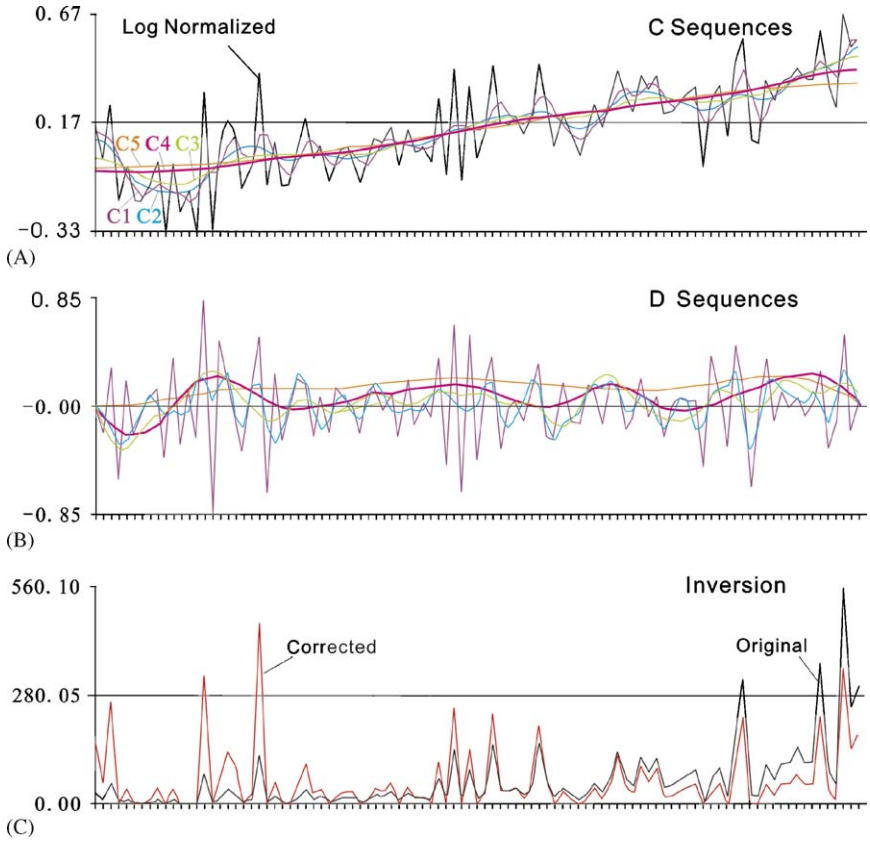

Fig. 7. Interference elimination of the CH_4 data for line 25 in the Yimeng Uplift of the Ordos Basin, China. The diagram A shows the decomposed continuous sequences such as C Sequences with log-normalization, the diagram B the detailed sequences such as D Sequences and the diagram C the corrected data with original data.

4. Univariate anomaly recognition

The common terms used to define seepage types are macro- and micro-seepage (Abrams, 1992, 2005). Micro-seepage refers to low concentrations of migrating hydrocarbons, not visible—but detectable—with standard analytical procedures. Migration mechanisms commonly proposed for micro-seepage include buoyancy of micro-bubbles (Price, 1986; Zhang, 1993; Klusman and Saeed, 1996; Zhang and Liao, 1998; Saunders et al., 1999; Brown, 2000; Zhang and Bai, 2002; Zhang, 2003; Abrams, 2005). Macro-seepage usually refers to large concentrations of migrating hydrocarbons, which are generally visible and related to bulk flow (Zhang, 1993; Abrams, 2005). But macro-seepage anomalies are not common in most geochemical surveys. In reality, there exists another type of non-visible anomalies well developed over faults. Their intensities lie between micro-seepage and macro-seepage anomalies, and referred to as seepage anomalies (Zhang, 1993; Zhang and Liao, 1998; Zhang and Bai, 2002; Zhang, 2003). The seepage anomalies result from deep basin water and/or ultra-small gas bubbles migrating towards the surface along fault planes. In many geochemical surveys, there exist both micro-seepage and seepage anomalies. Micro-seepage anomalies directly reflect oil/gas fields, and seepage anomalies are related to structures such as faults (Fig. 8, Zhang, 1993; Zhang and Liao, 1998). The geochemical prospecting method varies with the types of anomalies so that these two distinct types of anomalies need to be separated. Because the traditional statistical methods are unable to distinguish between these types of anomalies, Price (1986) concluded that direct geochemical exploration methods for hydrocarbons are not recommended in tectonically active areas, and Tompkims (1990) considered that geochemical surveys can only provide general indications. However, if one can distinguish the two types of anomalies, the surface geochemistry might be useful, even in tectonically active areas. The recognition methods for univariate anomalies documented in Zhang and Liao (1998) were successfully used for this distinguishing in some areas but cannot be applied in this study area as the data do not show any turning points on the cumulative probability graphs (Fig. 9).

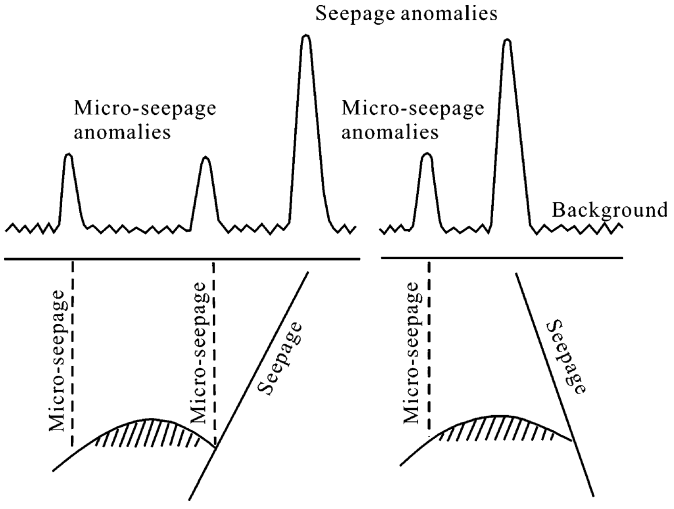

Fig. 8. Model of the types of hydrocarbon anomalies and their formation mechanisms (after Zhang (1993); Zhang and Liao (1998)).

The multi-fractal model (Cheng et al., 1994; Cheng, 1999), developed for metal exploration, can be adapted for hydrocarbon exploration if the data fit it. This model employs log–log plots for element concentration-area to separate anomalies from background. In this paper, the elements are replaced as hydrocarbons. The model can be described as

$$A(\geqslant\rho) \propto \rho^{-\beta}, \tag{1}$$

where $A(\geqslant\rho)$ represents the area enclosed by contours which has contour values greater than or equal to (ρ), and β is an exponent which assumes different values for sets of contours corresponding to different ranges of geochemical data. Assuming that in a study area the sampling is at a constant spacing or even grid, $N(\geqslant\rho)$ can statistically represent the number of samples in $A(\geqslant\rho)$, then

$$N(\geqslant\rho) \propto A(\geqslant\rho), \tag{2}$$

$$\because P(\geqslant\rho) \propto N(\geqslant\rho) \text{ and } P(\geqslant\rho) = 1 - P_c(<\rho), \tag{3}$$

$$\therefore [1 - P_c(<\rho)] \propto \rho^{-\beta}, \tag{4}$$

where $P(\geqslant\rho)$ is the probability of samples with values equal to and greater than (ρ); $P_c(<\rho)$ represents cumulative probabilities less than the value of (ρ). If we sort the geochemical data for a univariate in the increasing order and get a sequence x_j ($j = 1, 2, \ldots, n$; n is the number of the samples), we can replace x_j as (ρ) and P_{cj} as $P_c(<\rho)$ assuming that contours are plotted at the values of x_j ($j = 1, 2, \ldots, n$), then

$$(1 - P_{cj}) \propto x_j^{-\beta} \quad j = 1, 2, \ldots, n. \tag{5}$$

From this formula, sample points can be conveniently and easily plotted on the log-log graphs of $(1 - P_{cj})$ and x_j so as to accurately show the turning points of the curves. Generally, each population plots as one segment.

Fig. 9 also shows the log $(1 - P_{cj})$ and log x_j plots of the interference-eliminated data. The turnings are the corresponding limits between background, micro-seepage and seepage anomalies. All these limits of gaseous hydrocarbons are listed in Table 2. Using these limits, we plotted the counter maps of the acid-extractable hydrocarbons, as shown in Fig. 10. The seepage anomalies have evident linear features along the northeast and northwest directions, indicating these anomalies could reflect some underground geological features. However, these maps are very noisy. As the noises and anomalies are both in the high-frequency domain, the frequency filtering for noise reduction may eliminate the potential target anomalies and thus cannot be used here.

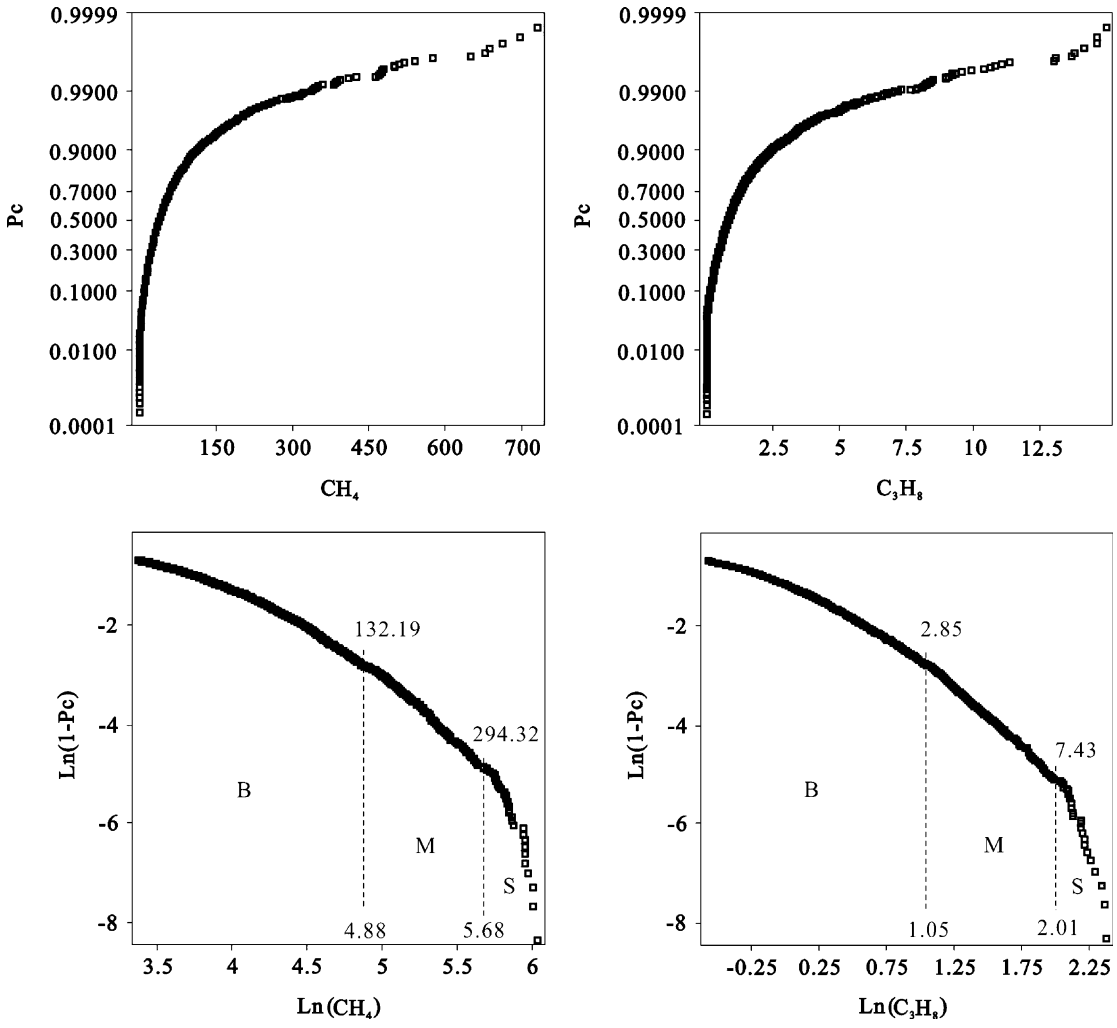

Fig. 9. Probability graphs and ln $(1-P_c)$ ~ln x plots of CH_4 and C_3H_8 for the Yimeng Uplift of the Ordos Basin, China, after the interference elimination. The units of hydrocarbon contents are μl/kg. The volumes in the units are those at 25 °C and 1 atm. P_c = cumulative probability; B = background; M = micro-seepage anomaly; S = seepage anomaly.

Table 2
Univariate limits for background, micro-seepage and seepage anomalies in the Yimeng Uplift of the Ordos Basin, China, after the interference was eliminated

	CH_4	C_2H_6	C_3H_8	iC_4H_{10}	nC_4H_{10}
Limits between background and micro-seepage anomalies	132	6.0	2.9	0.65	1.0
Limits between microseepage and seepage anomalies	294	19.9	7.4	2.5	2.9

5. Multivariate anomaly recognition

It is mathematically demonstrated that much of the problem involved in univariate anomaly recognition could be corrected by statistical multivariate anomaly recognition if the multi-normality is met (Zhang and Liao, 1998). Zhang and Bai (2002) reviewed the methods for multivariate recognition and proposed an artificial neural network (ANN)-based method if the multi-normality is not met. The training set for the BP-ANN is very important. As the micro-seepage anomalies typically are ring- or arc-shaped, they generally do not appear at the sites of oil/gas discovery wells. The samples at the well sites probably belong to background. The oil/gas discovery wells and hydrocarbon accumulations, therefore, could not be taken as the criteria for the establishment of the training set. Furthermore, no hydrocarbon accumulations were found prior to the geochemical survey in some areas. For this reason, the logic multiplication cluster analysis was established for the training set (Zhang and Bai, 2002). It was assumed that, if a given sample belongs to population i ($i = 0, 1, 2, \ldots, g-1$; g = the number of populations) in each geochemical univariate space of a variable association, the sample belongs to population i in the multivariate

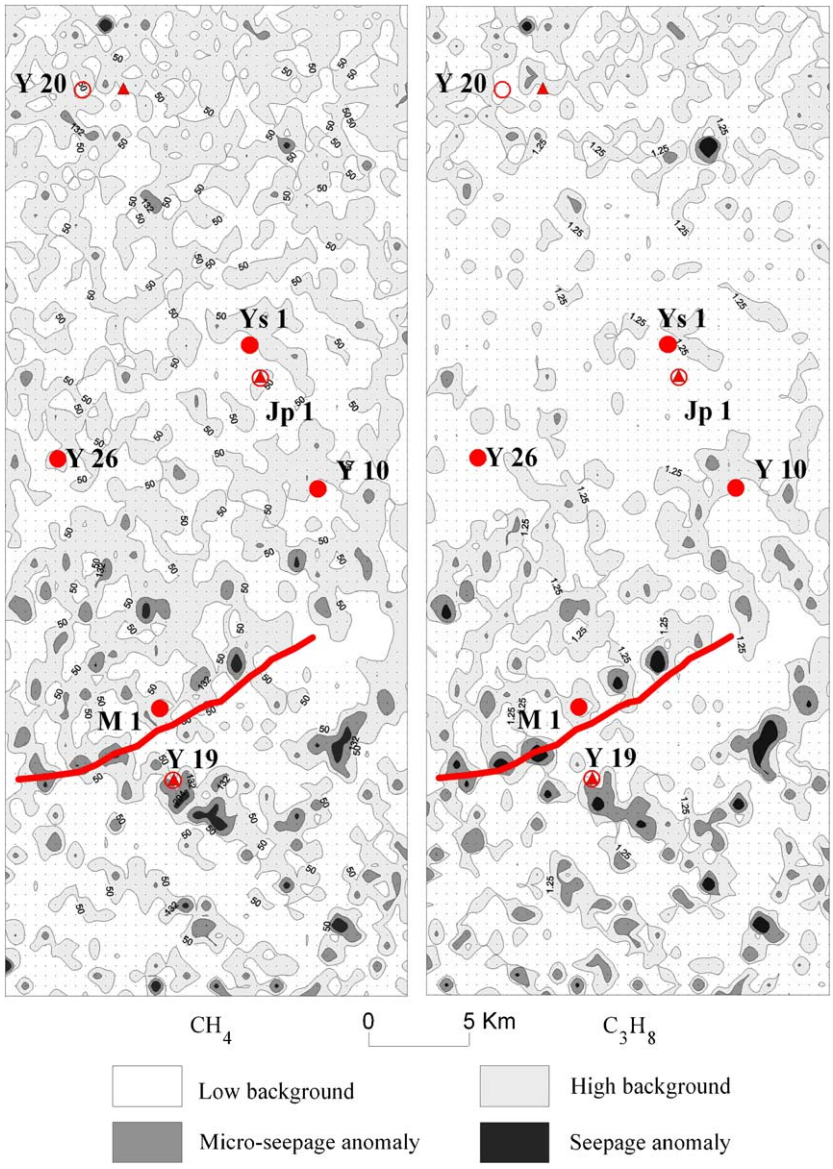

Fig. 10. Micro-seepage and seepage anomalies of acid-extractable CH_4 and C_3H_8 in the study area of the Ordos Basin, China, after interference elimination.

space of the association. If this logic multiplication is performed between each pair of geochemical variables, a table will be generated with the numbers of samples belonging to the corresponding populations for the pair of variables. This table is referred to as the matrix of logic multiplication. The logic multiplication results from the data in this study are listed in Table 3.

In this paper, the logic multiplication is studied again with the set theory. Assuming that population i ($i = 0, 1, 2, \ldots, g-1$; $g =$ the number of populations) in each geochemical univariate space of a variable association is set S_j ($j = 1, 2, 3, \ldots, m$; $m =$ the number of variables in a variable association), $\cap_{j=1}^{m} S_j$ belongs to the population i in the multivariate space of the association. The logic multiplication for the population i performed between each pair of geochemical variables provides $S_j \cap S_k$ ($k = 1, 2, 3, \ldots, m$; $k \neq j$). Table 3 actually is the list of the values of $|S_j \cap S_k|$. For variables j and k, the values of $|S_j \cap S_k|$ can illustrate relativities if the values of $|S_j| + |S_k|$ do not change with j and k. But they do in reality (Table 3). Considering that $|S_j| + |S_k|$ contains two of $|S_j \cap S_k|$s, the relative values, referred to as the correlation coefficients of

Table 3
Logic multiplication results for the two distinct anomalies of the study area in the Yimeng Uplift of the Ordos Basin, China

	SC1	SC2	SC3	SIC4	SNC4	SC1	SC2	SC3	SIC4	SNC4
SC1	281					23				
SC2	213	306				13	23			
SC3	161	209	276			20	22	49		
SIC4	178	186	153	413		11	17	24	48	
SNC4	113	127	115	136	392	15	17	30	17	87

logic multiplication in this paper, are defined to be

$$\gamma_{j,k} = 2\frac{|S_j \cap S_k|}{|S_j| + |S_k|}, \quad j = 1, 2, 3, \ldots, m; \quad k = 1, 2, 3, \ldots, m; \quad j \neq k. \tag{6}$$

From Table 3, $\gamma_{j,k}$ can be calculated using Formula (6) (see Table 4). Logic multiplication trees are established from the correlation coefficients in Table 4 by the same methods used to establish trees in the traditional cluster analysis. The associations of geochemical variables can be obtained from these trees. Fig. 11 illustrates that the correlation coefficients of logic multiplication for both micro-seepage anomalies and seepage anomalies decrease with the increase of variable numbers included in the logic multiplication. This suggests that not all of the variables are interrelated with respect to the description of one given population in some cases. Some may describe another population or there may be problems in the quality of the data. For micro-seepage anomalies in Fig. 11, CH_4, C_2H_6 and C_3H_8 are closely related but nC_4H_{10} and iC_4H_{10} are not related with them. For seepage anomalies, there is a great decrease in the correlation coefficients if nC_4H_{10} and iC_4H_{10} are included in the association. The variable association, therefore, includes CH_4, C_2H_6 and C_3H_8. The logic multiplication with these three variables produces the training set.

These two trees are different, probably because of the formation mechanisms for the two types of anomalies (Fig. 11). For micro-seepage (Price, 1986; Zhang, 1993; Klusman and Saeed, 1996; Zhang and Liao, 1998; Saunders et al., 1999; Brown, 2000; Zhang and Bai, 2002; Zhang, 2003; Abrams, 2005), CH_4, C_2H_6 and C_3H_8 are very mobile whereas nC_4H_{10} and iC_4H_{10} are less mobile. Separation might occur while gaseous hydrocarbons were moving up from oil/gas pools. Therefore, CH_4, C_2H_6 and C_3H_8 are more related in the tree of micro-seepage anomalies but nC_4H_{10} and iC_4H_{10} are not. For seepage (Zhang, 1993; Zhang and Liao, 1998; Zhang and Bai, 2002; Zhang, 2003), CH_4, C_2H_6, C_3H_8, nC_4H_{10} and iC_4H_{10} could all easily move upwards along fault planes so that they are related in the tree for the seepage anomalies.

The topology of the back propagation ANN (Fig. 12), the node characteristics or transfer function, connection weights and internal thresholds of the network are determined via the training set, by using the approach documented in Zhang and Bai (2002). It can be used directly for recognition simply by feeding the input vectors at the input nodes and selecting the output node with the highest value.

In order to illustrate the recognition results on contour maps, the integrated parameters are set up with the same methods for statistical methods (Zhang and Liao, 1998; Zhang and Bai, 2002). Assuming that there are g output nodes corresponding to g groups (populations) $G_i (0 \leqslant i \leqslant g-1)$ and that for a given subscript $i (0 \leqslant i \leqslant g-1)$, $iMax$ is the subscript corresponding to the node with the maximum output $Out_j (0 \leqslant j \leqslant g-1, j \neq i)$, then

$$Out_{iMax} = \max_{o \leqslant j \leqslant g-1, j \neq i} \{Out_j\}. \tag{7}$$

Table 4
Correlation coefficients of logic multiplication for the two distinct anomalies of the study area in the Yimeng Uplift of the Ordos Basin, China

	SC1	SC2	SC3	SIC4	SNC4	SC1	SC2	SC3	SIC4	SNC4
SC1	1					1				
SC2	0.73	1				0.57	1			
SC3	0.58	0.72	1			0.56	0.61	1		
SIC4	0.51	0.52	0.44	1		0.31	0.48	0.49	1	
SNC4	0.34	0.36	0.34	0.34	1	0.27	0.31	0.44	0.25	1

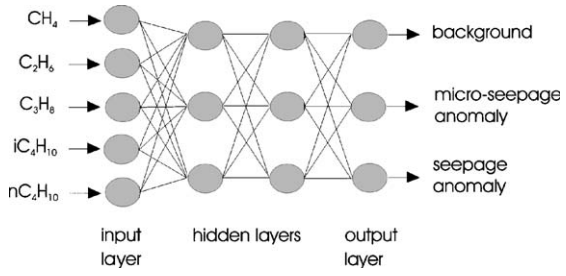

Fig. 12. The structure of the BP-ANN used for multivariate recognition of acid-extractable hydrocarbon anomalies in the study area of the Yimeng Uplift in the Ordos Basin, China.

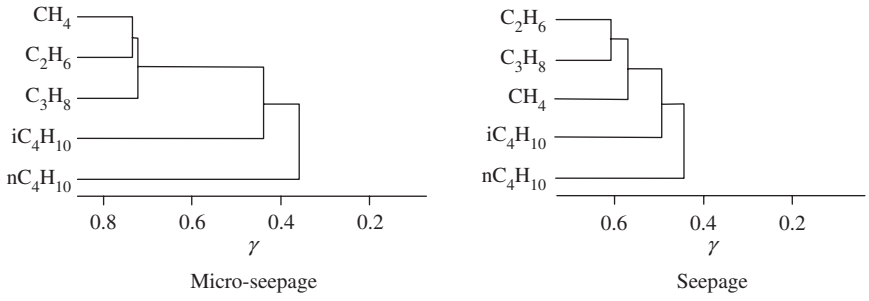

Fig. 11. Trees of logic multiplication for micro-seepage and seepage anomalies of the study area in the Yimeng Uplift of the Ordos Basin, China.

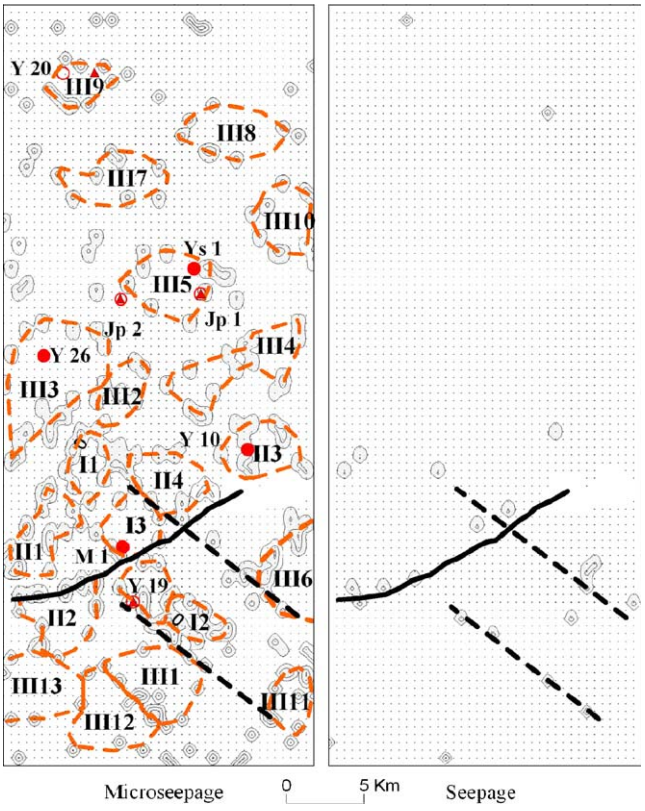

Fig. 13. Multivariate anomalies of gaseous acid-extractable hydrocarbons of the study area in the Yimeng Uplift of The Ordos Basin, China.

The integrated parameter for multivariate anomaly recognition using BP-ANN is designed as

$$NN_{Ci} = \frac{Out_i - Out_{iMax}}{Out_i + Out_{iMax}} \quad i = 0, 1, 2, \ldots, g-1. \tag{8}$$

The boundary between G_i and G_{i-1} or between G_i and G_{i+1} (G_{iMax} is G_{i-1} or G_{i+1}), the upper and lower limits of the corresponding transition zone are described by

$$NN_{CL} = 2K - 1. \tag{9}$$

If $K = 0.5$, NN_{CL} is the boundary; if $K = \alpha$ and $\alpha \neq 0.5$, NN_{CL} is the upper limit; if $K = 1 - \alpha$ and $\alpha \neq 0.5$, NN_{CL} is the lower limit. α is a confidence factor, $\alpha \in (0.5, 1)$. The concept of transition zone between populations is documented in Zhang and Liao (1998), and Zhang and Bai (2002). As for the data of this paper, we calculated NN_{C1} for micro-seepage anomalies and NN_{C2} for the seepage anomalies. The corresponding anomaly maps are plotted in Fig. 13.

6. Results

An anomalous zone, related to a single source, may be composed of a series of smaller anomalies forming a discontinuous pattern. The discontinuity in Fig. 13 can be caused by such factors as high ground noise, analytical errors, less optimum survey grid layout and/or uneven geological conditions. Before the interpretation of the anomalous patterns, their component anomalies should be reassembled. These components to be reassembled must meet the following criteria (Zhang and Liao, 1998; Zhang and Bai, 2002):

(1) Anomaly type (micro-seepage or seepage) for each component must be the same.
(2) Each component should be from a single oil/gas accumulation or another kind of single source. This is determined by similar ratios of paired variables. Q-mode cluster analysis of the paired variable ratios can help to determine whether the smaller anomalies are derived from a single source or not. Evidently, this operation needs more geochemical variables such as gas hydrocarbons, liquid hydrocarbons and isotopes.
(3) Each component should be spatially near one another on the anomaly map.
(4) The overall shape of the assembled anomalous zone must correspond to the mechanism which leads to its formation: (a) micro-seepage anomalous zones over oil/gas accumulations are ring-, arc- or irregularly-shaped; (b) seepage anomalous zones display belt-, string-bead- or irregularly shaped patterns over faults.

This combination of anomalies is conducted for the micro-seepage and seepage anomalies (Fig. 13). Due to a lack of liquid hydrocarbon and carbon isotope data, however, chemical composition of anomalies and its relationship with isotopes are not analyzed. The seepage anomalies recognized in this paper show evident linear features. One of the string-bead anomaly zones is coincident with the large fault recognized on the seismic sections. This fault controls hydrocarbon migration and accumulation (Sun et al., 2000). In addition to the seepage anomaly zones trending the NE–SW direction, the other seepage anomaly zones trend in NW–SE direction. In the Ordos Basin, the faults usually have smaller throws so that it is difficult to recognize them on seismic sections. The seepage anomalies may provide a clue that can help to identify these kinds of faults. The faults related with the seepage anomalies are important as they usually have a genetic relationship with petroleum entrapment.

Micro-seepage anomaly halos can reflect approximate locations of petroleum accumulations, as shown in Fig. 8. The micro-seepage anomalies recognized in this paper are mostly ring-shaped halos that are different from the anomalies previously recognized with traditional methods (Figs. 4 and 13). These anomaly halos are seemingly distributed irregularly. However, there are more anomalies close to the large fault. This suggests that this fault may have acted as an important pathway of migration and led to the entrapment of hydrocarbons in the Early Cretaceous. Extensive distribution of source rocks and sand bodies in the Ordos Basin may have resulted in abroad distribution of oil/gas pools. The distribution of the micro-seepage anomaly rings may be also controlled by the NW–SE trending faults (Fig. 13). The anomaly halos

correspond to structural traps whereas the other anomalies imply that there exist numerous subtle traps in the study area. In the Ordos Basin, the subtle traps are the main trap style for entrapping oil/gas.

The anomaly halos are small in scale, which accords with the sizes of the traps in this study area (Figs. 3 and 13). Ys 1, Y 10, Y 26 and M 1 wells with commercial flows are located within the anomaly halos I3, III3, III4 and III5. Jp 1, Jp2 and Y 19, wells with sub-commercial flows are at the edges of anomaly halos III5 and Y 19 respectively. These correlations illustrate that the traps with these halos contain hydrocarbons. Although the well Y 20 is dry, an oil macro-seepage was found at the surface. The existing wells with commercial and sub-commercial flows further demonstrate that the halos of micro-seepage anomalies can indicate whether the traps contain hydrocarbons or not. The halos of micro-seepage anomalies I2, II2, II4 and III2 are coincident with structural traps (Figs. 4 and 13) and they have not been drilled yet. A greater attention should be paid to these halos in the future exploration. The small size of the anomaly halos in the study area suggests that there is little potential to find large-scale pools in the study area but there may exist numerous small pools which are close to one another. Thus, there is still exploration potential in the study area. Further studies tackling the local geology are required for all of the anomaly halos.

7. Summary

In the southern part of the study area, the anomalies recognized using typical statistical methods are masked by the interference from the variation of soil composition. The interference also resulted in wrong interpretation of anomalies in the northern part of the study area. The method for interference elimination used in this paper can solve this problem. Hydrocarbon composition is not used to study the features of the anomalies, as the values of hydrocarbon contents were greatly varied when interference was eliminated.

The typical statistical methods cannot be always applied to successfully process the geochemical data for hydrocarbon exploration. This paper employed the multi-fractal model and adapted logic multiplication cluster analysis, which can be applied to univariate anomaly recognition and multivariate anomaly recognition, respectively. The anomalies obtained with the new methods coincide with oil/gas fields and faults. The micro-seepage anomalies are mainly distributed in the locations close to the large fault and suggest there exists exploration potential. Four of the micro-seepage anomaly halos coincide with structural traps. It is recommended to conduct detailed geological research on them. The micro-seepage anomalies also suggest that there probably exist plenty of subtle traps. We recommend to investigate the sequence stratigraphy of the study area. The seepage anomalies show that there are minor NW–SE trending faults. Considering the close relationships between faults and hydrocarbons, we also recommend to restudy the seismic sections to verify their existence. Following these comprehensive studies, the anomaly halos should be ranked and the favorable ones should be tested by drilling

Since 1930s, plenty of acid-extractable hydrocarbon data have accumulated at least in China. Over a long period of time, these data have been directly and simply used and some of their prospecting results have not been successful. The application of the new methods can enhance the prospecting effectiveness of acid-extractable hydrocarbons and thus these data can be put into effective use than before.

Acknowledgements

We acknowledge the encouragement of Professors Tianjian Ruan and Qi Fei for the study of the data-processing methods. This study was financially supported by China National Major Science (973) Project (no. 2003CB214608).

References

Abrams, M.A., 1992. Geophysical and geochemical evidence for subsurface hydrocarbon leakage in the Bering Sea, Alaska. Marine and Petroleum Geology Bulletin 9, 208–221.

Abrams, M.A., 2005. Significance of hydrocarbon seepage relative to petroleum generation and entrapment. Marine and Petroleum Geology 22, 457–477.

Brown, A., 2000. Evaluation of possible gas microseepage mechanisms. Association Petroleum Geochemical Exploration Bulletin 84 (11), 1775–1789.

Cheng, Q., 1999. Spatial and scaling modeling for geochemical anomaly separation. Journal of Geochemical Exploration 65, 175–194.

Cheng, Q., Agterberg, F.P., Ballantyne, S.B., 1994. The separation of geochemical anomalies by fractal methods. Journal of Geochemical Exploration 51, 109–130.

Davidson, M.J., 1994. On the acceptance and rejection of surface geochemical exploration. Oil & Gas Journal 94 (23), 70–76.

Fu, C., Hu, W., Li, W., Zhao, Z., 2001. Research of the Deep Basin Gas in the Ordos Basin. Petroleum Industry Press, Beijing, pp. 1–243.

Gonzalez, F., Aldana, M., Costanzo-Aalvarez, V., Diaz, M., Romero, I., 2002. An integrated rock magnetic and EPR study in soil samples from a hydrocarbon prospective area. Physics and Chemistry of the Earth 27, 1311–1317.

Horvitz, L., 1939. On geochemical prospecting—I. Geophysics 4 (2), 210–229.

Horvitz, L., 1972. Vegetation and geochemical prospecting for petroleum. AAPG Bulletin 56 (5), 925–940.

Horvitz, L., 1985. Geochemical exploration for petroleum. Science 229 (4716), 821–827.

Klusman, R.W., 1993. Soil Gas and Related Methods for Natural Resource Exploration. Wiley, New York, pp. 1–112.

Klusman, R.W., Saeed, M.A., 1996. A comparison of light hydrocarbon microseepage mechanisms. In: Schumacher, D., Abrams, M.A. (Eds.), Hydrocarbon Migration and its Near Surface Effects, vol. 66. AAPG Memoir, pp. 157–168.

Li, L., Yuan, Z., Hui, K., Liu, S., 2000. Accumulation regulation of upper Paleozoic gas in the northern Ordos Basin. Oil and Gas Geology 21 (3), 268–271 (in Chinese with English abstract).

Price, L.C., 1986. A critical overview and proposed working model for surface geochemical exploration. In: Davision, M.J. (Ed.), Unconven-

tional Methods in Exploration for Petroleum and Natural Gas (IV). Southern Methodist Univ. Press, Dallas, pp. 1–30.

Ritts, B.D., Hansonb, A.D., Darbyc, B.J., Nansona, L., Berry, A., 2004. Sedimentary record of Triassic intraplate extension in North China: evidence from the nonmarine NW Ordos Basin, Helan Shan and Zhuozi Shan. Tectonophysics 386, 177–202.

Ruan, T., Cheng, J., 1991. Hydrogen stripping of adsorbed hydrocarbons in soil sample—a new method in goechemical exploration for oil and gas. Journal of Southeast Asian Earth Science 5 (1–4), 5–7.

Ruan, T., Fei, Q., 1992. Exploration Geochemistry for Oil and Gas. The Press of China University of Geosciences, Wuhan, pp. 1–120 (in Chinese).

Saunders, D.F., Burson, K.R., Thompson, K., 1999. Model for hydrocarbon microseepage and related near-surface alternation. AAPG Bulletin 83 (1), 170–185.

Sun, C., Wang, F., Li, S., Rong, F., Tang, J., 2000. Geochemical prospecting in the Hangjinqi area of the northern Ordos Basin. Research Report of Geochemical Prospecting Center, SinoPec, pp. 7–16, unpublished.

Tedesco, S.A., 1995. Surface Geochemistry in Petroleum Exploration. Chapman & Hall, New York, pp. 1–125.

Tompkims, R., 1990. Direct location technologies: an unified theory. Oil & Gas Journal 88 (39), 126–134.

Xu, W., 1993. Near-surface geochemical prospecting study on the southern slope of Dongying Depression. Geophysical and Geochemical Exploration 17 (2), 81–88 (in Chinese).

Yang, H., Zhang, J., Wang, F., Wang, H., 2000. Characteristics of Paleozoic gas system of the Ordos Basin. Natural Gas Industry 20 (6), 7–11 (in Chinese with English abstract).

Yang, J., Li, K., Zhang, D., Zhang, S., Liu, S., 1992. Petroleum Geology of China, Changqing Oil Field, vol. 12. Petroleum Industry Publishing House, Beijing, 490pp.

Zhang, L., 1993. A primary study of the method for the recognition of anomalies in geochemical hydrocarbon exploration. In: Proceedings of the Third Chinese Geochemical Hydrocarbon Exploration Symposium, pp. 55–62.

Zhang, J., Chang, X., 2002. Theory of Deep Basin Gas and Its Application. Geological Press, Beijing, pp. 86–87 (in Chinese).

Zhang, L., 2003. Vacuum desorption of light hydrocarbons adsorbed on soil particles: a new method in geochemical exploration for petroleum. AAPG Bulletin 87 (1), 89–97.

Zhang, L., Bai, G., 2002. Application of the artificial neural network to multivariate anomaly recognition in geochemical exploration for hydrocarbons. Geochemistry: Exploration, Environment, Analysis 2, 75–82.

Zhang, L., Liao, Z., 1998. A study of the method for the recognition of anomalies in geochemical hydrocarbon exploration. Journal of China University of Geo-sciences 9, 72–80.

Zhang, L., Bai, G., Xu, Y., 2003. A wavelet-analysis-based new approach for interference elimination in geochemical hydrocarbon exploration. Mathematical Geology 35 (8), 939–952.